Optimal Transmission Line Coupling Generation System Design for Rural Electrification

J. S. Chaves, J. S. Acosta, and M. C. Tavares, *Senior Member, IEEE*

***Abstract*—An electric potential appears at floating wires located within a strong electric field. This phenomenon can be used to supply small isolated communities situated close to Extra-High Voltage transmission lines. This non-conventional distributed generation system has been studied for the last years. However, to improve the power generation system the optimal position of the floating wires, number of wires used, bundle radius, and type of wires must be properly identified. This paper presents a mathematical model solved with genetic algorithm to design a collector system with optimized induced voltage and minimized project cost, identifying the optimal reactor used for voltage regulation. The algorithm was applied to design a collector system that can tap-off 100 kW from a 230 kV transmission line. The trade-off between objectives and the Pareto optimal solutions were evidenced via several simulations using the weighting sum approach. These results allowed to identify a final geometry according to a-posteriori designer preferences.**

***Index Terms*—Energy harvesting, genetic algorithms, optimization, power tap.**

I. Introduction

ELECTRIC field on high voltage transmission line (TL) produces free electrical charges in its surrounding. The charge quantity depends on the voltage level at the phase conductors. If a floating conductor is located within the electric field, an electrical potential will appear [1], promoting power generation without any physical connection with the transmission line. Thus, based on this induction effect, we propose to build a collector line (CL) within the electric field region to produce a non-conventional electric generation (extraction) system. The use of this coupling supply source, based on a natural capacitive divider, is a promissory alternative to electrify rural communities without electrical service, or with low quality access.

Some authors have proposed different electrification systems to electrify small loads close to transmission lines. The use of capacitive dividers connected directly to the phases is a solution to small loads, but may compromise the power system reliability [2].

Manuscript received September 27, 2019; revised May 12, 2020 and July 6, 2020; accepted August 5, 2020. Date of publication August 18, 2020; date of current version July 23, 2021. This work was supported by the Brazilian Institutions CAPES (code: 001), CNPq and FAPESP (Projects 2017/20010-1 and 2015/26096-0). Paper no. TPWRD-01102-2019. *(Corresponding author: J. S. Chaves).*

The authors are with the School of Electrical and Computer Engineering, University of Campinas, Campinas, SP 13083-852, Brazil (e-mail: jschavesh@gmail.com; jhairacosta@gmail.com; sctavares@unicamp.br).

Color versions of one or more of the figures in this article are available online at https://ieeexplore.ieee.org.

Digital Object Identifier 10.1109/TPWRD.2020.3017376

Usually, grounded shielding wires (SW) are designed to protect overhead TLs from lightning strikes. Extra High Voltage (EHV) and Ultra High Voltage (UHV) TLs typically use two shielding wires per transmission tower, either in single- or double-circuit. Since these wires are not meant to carry power, they are usually made of steel. Therefore, they have lower conductivity and are much cheaper than phase conductors. Normally, one of the shielding wires is an optical fiber composite ground wire (OPGW) that is used for telecommunication and line teleprotection [3]–[5]. An innovative electrification method was presented in the 80 s when insulated shielding wires were energized at distribution high voltage level, feeding remote communities at a maximum distance of 100 km [6]. In some cases, regular Extra High Strength (typical shielding wire) conductor was replaced by Penguin conductors [7] to reduce losses.

An alternative based on insulated sections of TLs' shielding wire was proposed by Hydro Quebec to feed small remote loads. This configuration behaves as a natural voltage divider. Insulated shielding wires (ISW) were used to supply microwave repeater and communication facilities in Canada [8]–[11]. The same system was also implemented in Peru to attend small rural communities [12], but it suffered problems of assembly and load increase, and eventually it was discontinued. This proposal was analyzed recently in [13]–[15]. However, the project implementation has major drawbacks as it would imply in interventions in the transmission line assets, which are often extremely delicate.

A new proposal to address the main characteristics of the Floating Wires idea without intervening in an already existent transmission line structure is the construction of a collector line in the TL right-of-way. And here comes a new problem: when the insulated shielding wires (ISW) were used to extract energy from TL electric field the ISW were already positioned, and the induced voltage value was imposed for that tower geometry. This is no longer a restriction when the collector line is designed. However, new questions arose: where to locate the collector line? How many conductors should be used, and what is the best bundle shape?

This paper presents how to optimize the collector line design, maximizing the induced voltage and reducing the project cost. A detailed mathematical model solved using genetic algorithms is presented.

The main contributions of this paper are as follows:

1) A cost effective methodology to attend small communities without affecting the existent transmission line assets.
2) A new mathematical model for the optimal collector line design.

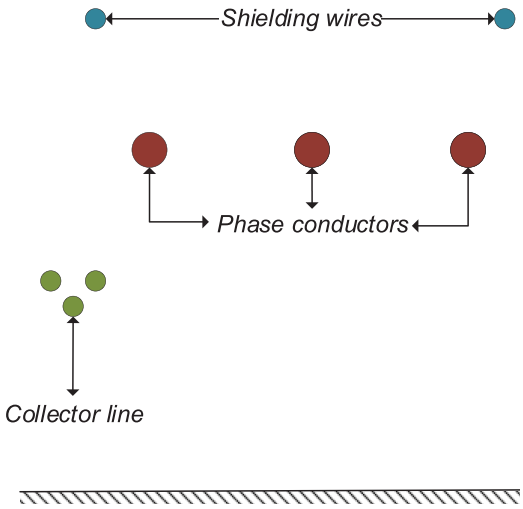

Fig. 1. Diagram of a high voltage line with a collector line in its right-of-way.

3) A straightforward methodology to help in the a-posteriori decision making process to choose the optimal collector line design.

II. Collector Line Design

Fig. 1 shows an example of the floating collector line located at the right-of-way of an extra-high voltage transmission line.

Considering the Maxwell potential equation, a matrix form can be written for a three-phase overhead transmission line with an additional wire d, using the superposition theorem as:

$$\vec{V} = \mathbf{P}\vec{Q} \tag{1}$$

$$\begin{bmatrix} V_a \\ V_b \\ V_c \\ V_{cl_{op}} \end{bmatrix} = \begin{bmatrix} P_{aa} & P_{ab} & P_{ac} & P_{ad} \\ P_{ba} & P_{bb} & P_{bc} & P_{bd} \\ P_{ca} & P_{cb} & P_{cc} & P_{cd} \\ P_{da} & P_{db} & P_{dc} & P_{dd} \end{bmatrix} \begin{bmatrix} Q_a \\ Q_b \\ Q_c \\ Q_d \end{bmatrix} \tag{2}$$

and

$$P_{kk} = \frac{1}{2\pi\varepsilon_0} \ln \frac{2h_k}{r_k} \tag{3}$$

$$P_{kn} = \frac{1}{2\pi\varepsilon_0} \ln \frac{D_{kn}}{d_{kn}} \tag{4}$$

where

- P_{kk} potential coefficient per unit length for the same conductor, F^{-1}-km
- P_{kn} potential coefficient per unit length between different conductors, F^{-1}-km
- h_k k conductor height, m
- r_k k conductor radius, m
- D_{kn} distance between conductor k to conductor n image, m
- d_{kn} distance between conductor k to conductor n, m
- Q_k electrical charge on conductor, C

Note that equation (2) can be expanded to include more circuits and sub-conductors. Since the values in $\mathbf{P}$ matrix derive only from the TL geometry, the induced voltage on the collector line is function of the voltage at phases' conductors and their position in space. Equation (2) is used to calculate the induced voltage on the collector wire. Note that the electrical charge on each phase of the TL is unknown, whereas the charge at a floating wire is null. Equation (5) presents a system with 4 variables and 4 equations, assuming $\mathbf{C}$ as the shunt capacitance matrix per unit of length of the transmission line. Equation (6) determines the induced voltage $V_{cl_{op}}$ that depends on the phase' voltage and the capacitance, which is a function of the geometry.

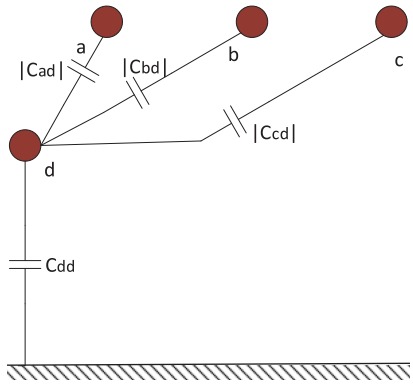

Fig. 2. Equivalent system (a). Equivalent capacitance of the power system. (b). Obtaining floating (collector) wires equivalent capacitance.

$$\begin{bmatrix} C_{aa} & C_{ab} & C_{ac} & C_{ad} \\ C_{ba} & C_{bb} & C_{bc} & C_{bd} \\ C_{ca} & C_{cb} & C_{cc} & C_{cd} \\ C_{da} & C_{db} & C_{dc} & C_{dd} \end{bmatrix} \begin{bmatrix} V_a \\ V_b \\ V_c \\ V_{cl_{op}} \end{bmatrix} = \begin{bmatrix} Q_a \\ Q_b \\ Q_c \\ 0 \end{bmatrix} \tag{5}$$

$$V_{cl_{op}} = -\frac{V_a C_{da} + V_b C_{db} + V_c C_{dc}}{C_{dd}} \tag{6}$$

Fig. 2 shows the equivalent capacitances of the system for the three-phase line represented in (2).

The voltage at collector line is calculated using (5) or (6). The equivalent capacitance between transmission line phases and the collector line C_{fd} is calculated in (7), whereas the equivalent capacitance between the collector line to ground C_{dg} is calculated in (8) [16].

$$C_{fd} = \sum_{n \in P_{h_1}} |C_{dn}| \longrightarrow P_{h_1} = \{a, b, c\} \tag{7}$$

$$C_{dg} = \sum_{n \in P_{h_2}} C_{dn} \longrightarrow P_{h_2} = \{a, b, c, d\} \tag{8}$$

Using the Thevenin theory, the total capacitance equivalent value is the sum C_{dg} and C_{fd} as shown in (9) where l_c is the total length of the collector line.

$$C_{eq} = (C_{dg} + C_{fd}) \cdot l_c \tag{9}$$

The Thevenin equivalent circuit impedance has a capacitive response. Note that the equivalent capacitance value is per unit of length, thus the power delivered is proportional to the collector line length.

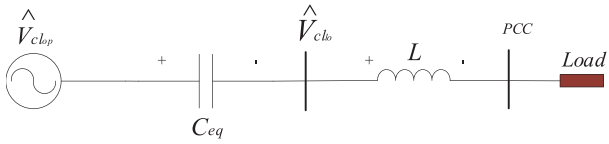

Fig. 3. Equivalent circuit system with the tuned reactor.

The presented system has a natural high impedance source value, that compromises the voltage regulation at the load. A strong source must have a low impedance to prevent large voltage deviation from nominal value during normal load variation. This is a naturally poor voltage regulated system that must be converted into a strong generation source.

To solve this problem we proposed to include a series inductive reactor with equal value to the source capacitive reactance. This will produce a series resonant circuit, reducing the impedance of the circuit.

The proposed method produces a strong power source at the point of common coupling (PCC), where the load or the rural feeder is connected (see Fig. 3).

The reactor can be calculated by the following equation:

$$L = \frac{1}{\omega^2 C_{eq}} \tag{10}$$

Through (10) it can be verified that the larger the collector line length the smaller the size of the tuning reactor. A way to reduce this value is by increasing the numbers of conductors on the collector line and the separation between them (bundle size), increasing the value of the capacitance (9). However, positioning the collector wires (CW) is not a straightforward procedure.

Therefore, we proposed to find the quantity, type and position of the conductors in the collector line through an optimization process in which the collector line length and the target tap-off power are fixed inputs, avoiding data dispersion on the results. These parameters are a designer choice that depends on the size of the community that will be attended, and the characteristics of the host transmission line.

The optimal position must attend some restrictions and objectives. In this way, the positioning of the parallel floating wires was obtained by solving an optimization problem related to maximizing the induced voltage on the parallel conductors, maximizing the equivalent capacitance C_{eq}, and minimizing the assembly costs, subjected to the following constraints:

- The transmission line shielding wires must shield collector line from lightning. The protection zone was identified with the electrogeometric model. As the shielding wires' positions are not changed, this identifies the feasible region for locating the collector wires.
- Collector line height cannot be higher than phases wires' height.
- Collector line's conductors cannot be under phase cables, avoiding any contact in the event of a fall. Also they cannot be positioned within the tower.
- The collector line height must respect the minimum distances to the ground at middle span.
- The magnitude of the electric field must not exceed the values that generate corona effect, considering both TL phases conductors and CW.
- The collector line conductors must respect the safety distance avoiding any touch with the phase conductor, even under wind effects.

III. Mathematical Model of the Optimization Problem

The optimal position, quantity, type of wires and bundle radius of the collector line are found by solving the mixed-integer nonlinear programming (MINLP) problem given by (11) to (26).

$$\max f = m_{obj_1} f_1 - m_{obj_2} f_2 - m_{obj_3} f_3 \tag{11}$$

where

$$f_1 = \frac{|V_{cl_{op}}|}{|V_{cl_{av}}|} - 1 \tag{12}$$

$$f_2 = \frac{P_{cl}}{P_{cl_{av}}} - 1 \tag{13}$$

$$f_3 = \frac{L_{tu}}{L_{tu_{av}}} - 1 \tag{14}$$

Subjected to restrictions in the objectives:

$$\sum_{obj=1}^{3} m_{obj} = 1 \tag{15}$$

Geometric restrictions:

$$\sqrt{(X_p - x_k)^2 + (Y_p - y_k)^2} > d_{\min} \tag{16}$$

$$\sqrt{(X_{\text{wind}} - x_k)^2 + (Y_{\text{wind}} - y_k)^2} > d_{\min} \tag{17}$$

$$|x_k| > |X_h| \tag{18}$$

$$|y_k| < |Y_l| \tag{19}$$

$$y_k > 5 \tag{20}$$

$$n_c < 8 \tag{21}$$

$$r_b < 0.5 \tag{22}$$

and electric restrictions

$$|V_{cl_{op}}| < 50 \tag{23}$$

$$|V_{cl_{op}}| \geq 10 \tag{24}$$

$$|V_{cl_{lo}}| < 60 \tag{25}$$

$$E_k < E_{\text{crit}} \tag{26}$$

where

$V_{cl_{op}}$	voltage on collector line in open circuit, kV
$V_{cl_{av}}$	voltage normalization constant, kV
P_{cl}	cost of collector line system, kUSD
$P_{cl_{av}}$	cost normalization constant, kUSD
L_{tu}	tuning reactor inductance, H
$L_{tu_{av}}$	inductance normalization constant, H
m_{obj}	simulation constant for objectives 1 to 3
X_p	x coordinate of phase wire, m
x_k	x coordinate of collector wire, m

Y_p y coordinate of phase wire, m
y_k y coordinate of collector wire, m
$d_{\min}$ minimum distance defined, in this paper 2, m
X_{wind} x coordinate of phase wire for wind effects, m
Y_{wind} y coordinate of phase wire for wind effects, m
X_h x coordinate of the phase wire with the longest distance to the tower center, m
Y_l y coordinate of the lowest phase wire, m
n_c collector wire bundle quantity
r_b radius of the bundle of the collector line, m
$V_{cl_{lo}}$ voltage on collector line with rural load, kV
E_k electric field on the surface of the k collector line wire, kV/m
E_{crit} minimum electric field to produce corona effect, kV/m

The collector line poles are supposed to be built at the same location as the host transmission line tower. This will take profit of already existent clean area, reducing construction cost.

The mathematical model is evaluated considering the conductors located in three scenarios: 1) at tower level, 2) mean height taking into account the sag, and 3) at mid-span. If a restriction in any scenario is not respected, then the solution is rejected.

The use of mean height value is adequate to calculate the induced voltage (V_{cl}), as the distances between the floating collector wires and TL phase wires vary due to conductors' positions along the line. Small variation on the induced voltage will be analyzed in future research due to random movements of conductors produced by wind.

A. Objectives

The mathematical model of the induced voltage and the tuning reactor were presented in section II, meanwhile the cost function is presented below.

1) Cost Function: The cost of the collector line considered in this paper is calculated based on the price of: conductors, insulator chain, utility poles, cross-arms and spacer dampers. The total cost is calculated by (27)

$$C_t = C_c + C_i + C_p + C_{ca} + C_s \tag{27}$$

$$C_c = 1.1 \cdot nc \cdot l_c \cdot \frac{W_e}{Al_c} \tag{28}$$

$$C_i = (N_a \cdot C_{iu} + C_{ix}) \cdot Q_p \tag{29}$$

$$N_a = V_{cl_{lo}} \frac{D_f}{d_f} \tag{30}$$

$$D_f = \frac{D_{fo}}{\sqrt{\frac{3.92 \cdot b_p}{273+t}}} \tag{31}$$

$$log(b_p) = log(76) - \frac{h}{18336} \tag{32}$$

$$C_p = 1.1 \cdot y_k \cdot \pi \cdot 0.32^2 \cdot RC_c \cdot Q_p \tag{33}$$

$$C_{ca} = 0.09^2 \cdot (2 \cdot r_{cl} + di_m) \cdot Q_p \tag{34}$$

$$di_m = \frac{8 \cdot CFO}{1.1 \cdot 3400 - CFO} \tag{35}$$

$$CFO = \frac{V_f}{0.7} \tag{36}$$

$$C_s = \frac{0.1593 \cdot n_c^2 + 0.9733 \cdot n_c + 0.484}{1000} \cdot \frac{4 \cdot Al_c \cdot Q_p}{0.350} \tag{37}$$

where

C_t collector line total cost, $USD
C_c conductors total cost, $USD
C_i insulators total cost, $USD
C_p utility pole total cost, $USD
n_c number of conductors of the collector line
W_e conductor weight per kilometer, kg/km
Al_c aluminum cost per ton, set as 4000 in this paper, $USD/ton
N_a number of insulators per chain
C_{iu} unit price of the insulator, set as 6.9, $USD
C_{ix} fixed price of insulator accessories, set as 40, $USD
Q_p number of utility poles of the CL
D_f minimum recommended creepage distance, mm/kV
d_f minimum creepage distance of each insulator, mm
D_{fo} minimum specific creepage distance [16], mm/kV
b_p barometric pressure, cm Hg
t conductor temperature, °C
h altitude at sea level, m
RC_c reinforced concrete cost, $USD/m^3
r_{cl} collector line conductor radius, m
CFO insulator critical flashover voltage for the stricken phase, kV
V_f TL phase voltage, kV

B. Restrictions

1) Collector Line Sag and Wind Effect: In order to attend safety distances in a transmission line project, the conductor sag variation must be considered as a project variable. For high-temperature levels, there is an increase in conductor length and its mechanical tension reduces. A maximum temperature will result in a maximum sag. Considering typical air temperature, conductor current flux, and emergency conditions, the conductor temperature was set as 80 °C for phase conductor and 65 °C for shielding wires and collector wires.

Regularly, the temperature-tension change calculation is performed using the heat balance equation presented as following:

$$\frac{(\frac{\omega_2 \cdot s_p}{S_c})^2}{24 \cdot \sigma_2^2} - \frac{\sigma_2}{E} + \frac{\sigma_1}{E} - \frac{(\frac{\omega_1 \cdot s_p}{S_c})^2}{24 \cdot \sigma_1^2} = \alpha \cdot (t_2 - t_1) \tag{38}$$

where

ω_1 conductor weight per unit length, kg/m
ω_2 final conductor weight per unit length, kg/m
s_p horizontal distance between the towers, i.e. span, m
S_c conductor cross-sectional area, mm^2
E conductor elastic elongation coefficient, kg/mm^2
α linear expansion coefficient, $1/°C$
t_1 initial conductor temperature, set as 15° C, $°C$

t_2 final conductor temperature, $^\circ C$
σ_1 initial conductor stress $(\frac{T_0}{S_c})$, kg/mm^2
σ_2 final conductor stress, kg/mm^2
T_0 horizontal strength for EDS condition, 18% rated strength, kgf

The equation (38) must be solved to σ_1 using iterative methods, i.e., Newton method. Hence, assuming a unique tower height the conductor sag can be calculated as:

$$Sag = \frac{T_2}{\omega_2}\left(cosh\left(\frac{S_p \cdot \omega_2}{2 \cdot T_2}\right) - 1\right) \tag{39}$$

where, T_2 is horizontal strength for final conductor stress in kgf. Sag equation above presents ideal situations, assuming a condition where no wind is present and there is no effect of ice loading. However, there always exists a wind pressure on the conductor and ice loading is observed in cold countries. Due to Brazilian weather conditions no ice loading effect was considered, and only horizontal wind was taken into account.

In order to calculate the conductor swing angle the methodology presented in the Brazilian standard NBR 5422 [17] was used, as presented below:

$$\tan(\theta) = k_w\left(\frac{q_0 \cdot d}{\omega_1 \cdot (V/H)}\right) \tag{40}$$

where

k_w wind dependent constant
q_0 reference dynamic pressure, kgf/m^2
d conductor diameter, m
V/H relation between weight span and wind span, typical value taken: 0.8
θ conductor swing angle, $^\circ$

The constant k_w is given by the following formula:

$$k_w = 3.569e^{-S_w 0.1623} + 0.3039e^{-S_w 7.767 \cdot 10^{-5}} \tag{41}$$

The reference dynamic pressure is given by the equation:

$$q_0 = \frac{1}{2}\rho S_w^2 0.101972 \tag{42}$$

where

ρ specific air mass, kg/m^3
S_w wind speed, m/s

The specific air mass formula is given below:

$$\rho = \frac{1.293}{1 + 0.00367\,t}\left(\frac{16000 + 64\,t - h}{16000 + 64\,t + h}\right) \tag{43}$$

where

t air temperature, $^\circ C$
h average altitude of the line region, m

Finally, the actual conductor weight considering the wind effect must be calculated as:

$$\omega_2 = \sqrt{(\omega_1)^2 + (\omega_1\, tan(\theta))^2} \tag{44}$$

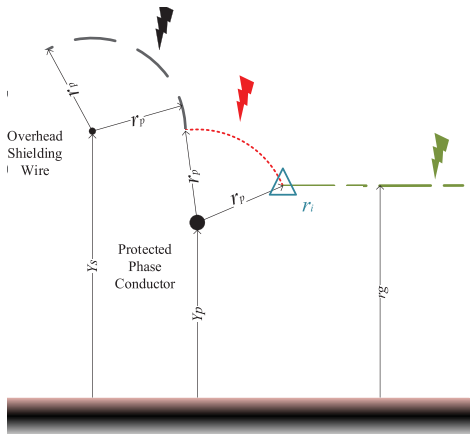

Fig. 4. Shielding failure striking distances for a two-conductor line.

Then, the conductor sag and the actual wire position under wind effects can be calculated. In this critical scenario, the phase conductors will move towards the CL wires.

2) Lighting Protection: As no change will be imposed to the existent TL, we identified a zone where the shielding wires protect the phase conductors and the collector line as well. Using the Electrogeometric Model presented in [18], the intersection between protection zone of phases' conductors or shielding wires (anyone farther from the centre of the TL) and the ground protection zone is identified, called as r_i, shown in Fig. 4. The collector line position must be farther from the point r_i at least a r_p distance to ensure adequate shielding protection for lightning. In order to calculate this region the following equations were used:

$$\sqrt{(r_i - x_k)^2 + (r_g - y_k)^2} > r_p \tag{45}$$

$$\sqrt{(-r_i - x_k)^2 + (r_g - y_k)^2} > r_p \tag{46}$$

$$r_p = 10\, I_c^{0.65} \tag{47}$$

$$r_g = [3.6 + 1.7\, ln(43 - y_c)]\, I_c^{0.65} \quad y_c < 40\ m \tag{48}$$

$$r_g = 5.5\, I_c^{0.65} \quad y_c \geq 40\ m \tag{49}$$

$$I_c = \frac{2\, CFO}{Z_1} \tag{50}$$

where:

x_k x coordinate of collector wire, m
y_k y coordinate of collector wire, m
r_p strike distance to phase wire, m
r_g strike distance to ground from leader tip, m
r_i intersection point to r_p and r_g, m
X_k x coordinate of phase wire, m
Y_k y coordinate of phase wire, m
I_c critical stroke current causing flashover, kA
y_c average height of lowest phase conductor, m
Z_1 TL positive sequence characteristic impedance, Ω

3) Conductor's Electric Field: The electric field on the surface of the k conductors on the tower are produced by their

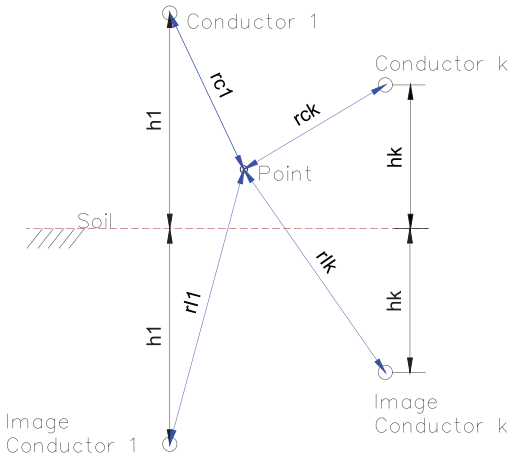

Fig. 5. Image method representation for electric field calculation.

electric charge q_k. The electric field can be calculated at any point p using the image method presented in Fig. 5, according to Eqs. (51) and (52). The electric field magnitude E_p at any point p is composed by the real and imaginary components of $\widetilde{E}_x$ and $\widetilde{E}_y$ as shown in (53).

$$\widetilde{E}_x = \sum_{k=1}^{n} \frac{q_k}{2\pi\varepsilon_0}\left(\frac{x_p - x_k}{r_c^2} - \frac{x_p - x_k}{r_I^2}\right) = E_{rx} + jE_{ix} \tag{51}$$

$$\widetilde{E}_y = \sum_{k=1}^{n} \frac{q_k}{2\pi\varepsilon_0}\left(\frac{y_p - y_k}{r_c^2} - \frac{y_p + y_k}{r_I^2}\right) = E_{ry} + jE_{iy} \tag{52}$$

$$E_p = \sqrt{E_{rx}^2 + E_{ix}^2 + E_{ry}^2 + E_{iy}^2} \tag{53}$$

where

$$r_c^2 = (x_p - x_k)^2 + (y_p - y_k)^2 \tag{54}$$

$$r_I^2 = (x_p - x_k)^2 + (y_p + y_k)^2 \tag{55}$$

In the above equations x_p and y_p are the x and y positions of a point p; x_k and y_k are the x and y positions of the k conductor; r_c in (54) is the distance between the conductor k and the point p; and r_I in (55) is the distance between the image of the conductor k and the point p.

If p is on the conductor surface then $E_{sup_k} = E_p$. The magnitude of E_{sup_k} defines the occurrence of the Corona effect, that depends on the environmental conditions and the wire characteristics, especially the external radius. Peek was the first to propose, from experimental studies, the critical electric field of conductors with small diameter [19]. Later studies developed by Miller [20] found that the conductor radius is more important than what was considered by Peek. Therefore, for an external diameter greater than 0.935 cm and lower than 6.8 cm, the critical electrical field (E_{crit_k}) is calculated by (56).

$$E_{crit_k} = 18.11 f_s \delta_{pa}\left(1 + \frac{0.54187}{\sqrt{R_k \delta_{pa}}}\right) \tag{56}$$

where

f_s Surface factor that is typically 0.82

Algorithm 1: Optimal Allocation of Insulated Wires.

```
Initialize parameters and limits
P_o ← N random solutions inside the feasible region
it ← 1
while it ≤ max(generations) do
    P_a ← N/10 random solutions in the feasible region
    P_o ← P_o ∪ P_a
    Evaluate all solutions in P_o
    P_o ← Natural selection of P_o
    S_o ← Crossover of P_o with 90% of probability
    S_o ← Mutation of S_o with 5% of probability
    P_o ← P_o ∪ S_o
    if it = max(generations) then
        Evaluate all solutions in P_o
        P_o ← Natural selection of P_o
    end if
    it ← it + 1
end while
```

δ_{pa} Atmospheric pressure, $mmHg$
R_k External radio of k conductor, cm

Since the electric field in the surface of the conductors is not uniform, different p points around each k conductors' surface were chosen and the point with the maximum electric field was selected as E_{sup_k}.

IV. Optimal Allocation of Insulated Wires

The MINLP problem presented in (11) is solved using a genetic algorithm (GA), a natural computing method based on the evolution of population of solutions, that is simple and widely used in different optimization problems [21]. Thus, a set of N possible solutions compound a population $\mathbf{P_o}$ as shown in (57). Each one of the $\vec{S}_n$ candidate solutions ($\forall n \in N$) is represented by a chromosome comprised by the variables shown in (58).

$$\mathbf{P_o} = \left\{\vec{S}_1, \ldots, \vec{S}_N\right\}^T \tag{57}$$

$$\vec{S}_n = \{x_{cIns}, y_{cIns}, n_c, r_{cl}, c_{ty}\} \tag{58}$$

where

x_{cIns} x coordinate of the insulated conductor, m
y_{cIns} y coordinate of the insulated conductor, m
n_c insulated wire bundle quantity
r_{cl} radius of the bundle of the collector line, m
c_{ty} conductor type of collector line

The general procedure used to optimize (11) follows the pseudo code presented in Algorithm 1. First, it is created an initial population $\mathbf{P_o}$ composed by N random solutions generated into the feasible region. Then, the algorithm begins the main optimization process, composed by the stages of insertion of new random solutions, evaluation of the solutions, natural selection, crossover and mutation. The stages are executed until the maximum number of generations is stabilized. Then, the final $\mathbf{P_o}$ is evaluated and the natural selection process is performed.

When working with GAs it is desired to explore the solution space as much as possible. However, because of the natural selection mechanism, the solutions tend to become similar over the time, degrading the ability of exploring new solutions. To overcome this there are different strategies like increasing the initial population size, choosing a natural selection procedure with low selective pressure, or introducing new random solutions to the population in each generation. Thus, to solve the problem the present algorithm introduces at each generation $\mathbf{P_o}$ a random population $\mathbf{P_a}$ with a size of 10% of $\mathbf{P_o}$, and uses a natural selection process with a slow selection pressure.

At each generation $N/10$ new random solutions are added to population $\mathbf{P_o}$ and a value calculated by (11) of each solution in $\mathbf{P_o}$ is obtained.

Afterwards, the new population $\mathbf{P_o}$ experiments a natural selection process and $\mathbf{P_o}$ is reduced to N solutions. The natural selection is performed through a modified tournament in which each solution faces 0.4 N random solutions in $\mathbf{P_o}$. The number of victories of each solution is counted and ranked. The N solutions with more victories remain in $\mathbf{P_o}$ and are denominated progenitors/parents, whereas the others are eliminated.

After natural selection an uniform crossover is performed over $\mathbf{P_o}$ and N descendants/sons are obtained comprising the population $\mathbf{S_o}$. In uniform crossover a random pair of parents have a probability of 90% (in this case) to produce two sons with combined genetic material.

As happens in nature, a genetic mutation can occur with low probability at any generation. Therefore, the population $\mathbf{S_o}$ can suffer a mutation with a probability of 5%. The mutation of continuous variables ($x_{cIns}, y_{cIns}, r_{cl}$) is performed by adding random numbers obtained with gaussians distributions with standard deviation of 0.1; whereas the mutation of integer variables (n_c, c_{ty}) is performed by adding random integers obtained with gaussians distributions with standard deviation of 1. After mutation, the new $\mathbf{P_o}$ will be composed by the union of the previous generation $\mathbf{P_o}$ (progenitors) plus the population $\mathbf{S_o}$ (descendants).

At this point, the population $\mathbf{P_o}$ has a size of 2 N that will be reduced to N in the next natural selection stage. This happens in the next generation or immediately if the algorithm is in the last generation.

In the end, almost all the solutions in $\mathbf{P_o}$ will be very similar and optimized.

Finally, to observe the trade-off between objectives the entire process is repeated several times with different values of $m_{obj_1}, m_{obj_2}, m_{obj_3}$. This is known as the weighting sum approach and allows to obtain different solutions according to the objectives' weight. The solutions obtained with this method are called Pareto optimal solutions and represent the best solutions for a certain weight of each objective. This approach helps in the a posteriori decision making process to select a solution according to the specific needs or limitations of the project.

V. Test and Results

The wire allocation algorithm was tested by designing an optimal collector line close to the 230 kV transmission line presented in Fig. 6. The use of a 230 kV transmission system was adopted because in most of the developing countries this is the highest available voltage level. The average span of the line is 350 m and a wind speed of 27.77 m/s was considered. The transmission line has a Z_1 equal to 268.26 Ω, $CFO = 198.27$ kV, and $I_c = 1.47$ kA.

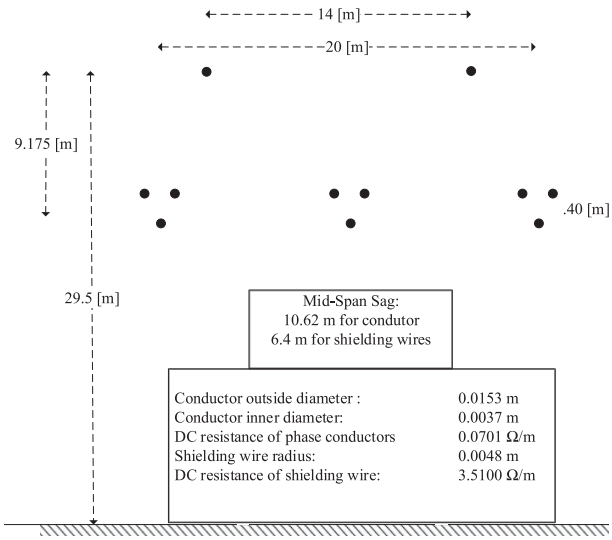

Fig. 6. Test 230-kV transmission line.

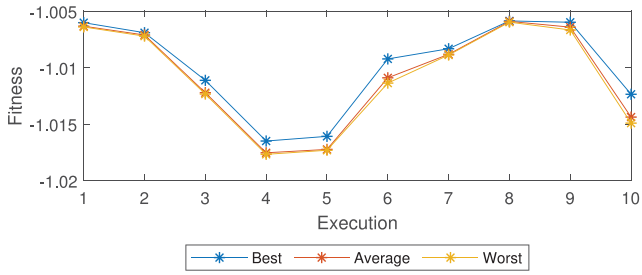

Fig. 7. Fitness behavior of the solutions for different runs considering $m_{obj_1} = m_{obj_2} = m_{obj_3} = 0.3333$.

In the optimization process 42 types of steel cable, named with the code t_c as presented in Table I, were considered as possible candidates for a 20 km collector line with a target load of 100 kW.

To show the repeatability of the solutions, using a population of 500 possible solutions and 40 generations, 10 runs with $m_{obj_1} = m_{obj_2} = m_{obj_3} = 0.3333$ were performed. As a result, Fig. 7 and Table II show that the mean value of the fitness is close to -1.01 with an small variance of $\sigma^2 = 3.51e^{-5}$. Accordingly, simulations with different $m_{obj_1}, m_{obj_2}, m_{obj_3}$ can be performed with the same population size $N = 500$ and the same number of generations $g = 40$.

From results in Table II, it is possible to observe that all the simulations found a solution using a bundle of three wires with values of $V_{cl_{op}}$, P_{cl} and L_{tu} around to 40 kV, 144.5 kUSD and 27 H, respectively.

TABLE I
CONDUCTORS USED FOR ALLOCATION ALGORITHM

t_c	Nominal diameter [mm]	DC resistance [Ω/km]	Standard weight [kg/km]
101	7.94	4.76	305
102	9.52	3.44	407
103	11.11	2.46	594
104	12.70	1.97	768
105	7.94	4.40	305
106	9.52	3.18	407
107	11.11	2.26	594
108	12.70	1.80	768
109	7.94	5.25	305
110	9.52	3.81	407
111	11.11	2.72	594
112	12.70	2.17	768
113	7.94	4.82	305
114	9.52	3.51	407
115	11.11	2.53	594
116	12.70	2.00	768
117	4.62	0.13	4170
118	4.11	0.17	3307
119	3.66	0.22	2622
120	3.26	0.27	2080
121	2.90	0.35	1649
122	2.58	0.44	1308
123	4.62	0.26	2128
124	4.11	0.34	1688
125	3.66	0.42	1339
126	3.26	0.54	1062
127	2.90	0.68	842
128	2.58	0.86	667.8
129	4.62	0.74	781.2
130	4.11	0.91	619.5
131	3.66	1.15	491.1
132	3.26	1.46	389.6
133	2.90	1.84	308.9
134	2.58	2.32	245.1
135	2.30	2.93	194.4
136	2.05	3.69	154.2
137	4.62	1.69	334.1
138	4.11	2.14	265
139	3.66	2.10	210.7
140	3.26	3.40	166.7
141	2.90	4.29	132.2
142	2.58	5.41	104.8

TABLE II
SOLUTION FOR 10 SIMULATIONS USING THE SAME m_{obj}.

x_k [m]	x_y [m]	n_c	r_b [m]	t_c	$V_{cl_{op}}$ [kV]	P_{cl} [k$USD]	L_{tu} [H]
12.92	15.52	3	0.492	105	40.05	129.81	26.74
12.88	15.59	3	0.419	105	40.57	129.94	27.35
12.89	15.44	3	0.470	105	39.80	129.64	26.92
12.89	15.30	3	0.499	105	39.14	129.36	26.71
12.88	15.33	3	0.481	101	39.32	129.41	26.84
12.97	15.52	3	0.499	101	39.73	129.79	26.72
12.92	15.47	3	0.498	105	39.82	129.70	26.69
12.92	15.52	3	0.499	105	40.01	129.80	26.68
12.92	15.52	3	0.498	101	40.01	129.80	26.69
12.95	15.59	3	0.419	101	40.19	129.94	27.42

Once the repeatability of the solutions was checked, 1000 simulations using random objective weights m_{obj} were performed to obtain the Pareto optimal solutions.

The simulations results in the objective space, i.e., space composed by the objective value of each individual, are presented in Figs. 8 and 9.

Fig. 8 shows a bi-objective representation of the solutions, in which column 1 shows the number of solutions in each objective value, whereas column 2 shows the trade-off of one objective relate to another. However, since the problem has three objectives, a clear Pareto front cannot be obtained in two dimensions, so the relationship between objectives presented in Fig. 8 is not so evident.

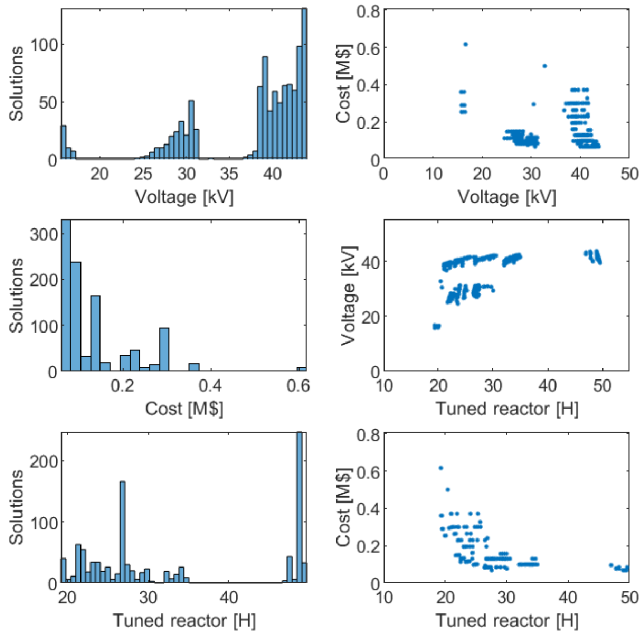

Fig. 8. Bi-objective representation of Pareto front.

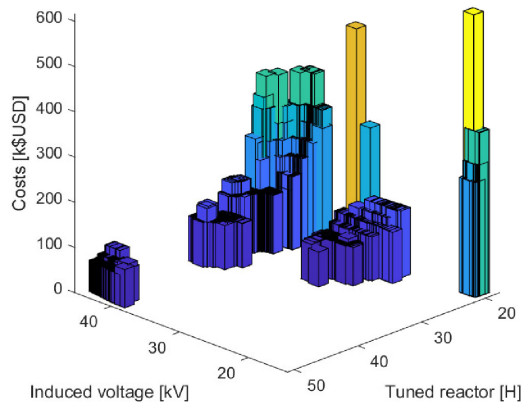

Fig. 9. Pareto front.

A better representation in a three-dimensional space is presented in Fig. 9. Now it is possible to see the trade-off of the three objectives at the same time. Some conclusions may be drawn: if a small tuned reactor is selected together with high induced voltage values, the cost of the project will increase. On the other hand, if lower costs are prioritized, it will be necessary to sacrifice either the induced voltage or the tuned reactor size.

Table III and Table IV compile some relevant results and simulation parameters. It can be seen that when the only goal is to reduce the tuned reactor ($m_3 = 1$) more n_c is required, significantly increasing the costs and reducing the induced voltage. When the only objective is to reduce costs ($m_2 = 1$) a lower quantity of conductors is necessary and the induced voltage is sacrificed. In the final extreme case, when the only objective is to

TABLE III
POSSIBLE SOLUTIONS OF DIFFERENT VALUES OF m_{obj}

m_1	m_2	m_3	V_{clop} [kV]	P_{cl} [k$USD]	L_{tu} [H]
0	0	1	16.68	616.8	19.314
0	1	0	41.26	67.94	49.153
0.093	0.726	0.180	43.53	68.75	48.948
0.374	0.254	0.371	40.23	129.8	26.973
0.376	**0.347**	**0.276**	**38.57**	**97.84**	**32.059**
0.387	0.143	0.468	39.15	195.3	23.062
0.047	0.749	0.203	30.44	84.18	26.685
0.487	0.465	0.046	42.20	68.55	49.142
0.916	0.071	0.011	42.99	77.34	47.831
1	0	0	43.08	95.46	47.024

TABLE IV
FITNESS SOLUTIONS OF DIFFERENT VALUES OF m_{obj}

m_1	m_2	m_3	x_k [m]	x_y [m]	n_c	r_b [m]	t_c
0	0	1	10.83	10.89	8	0.499	104
0	1	0	12.71	15.51	1	0.241	101
0.093	0.726	0.180	12.66	15.90	1	0.241	101
0.374	0.254	0.371	12.92	15.52	3	0.493	101
0.376	**0.347**	**0.276**	**13.00**	**15.32**	**2**	**0.497**	**101**
0.387	0.143	0.468	13.04	15.48	5	0.498	101
0.047	0.749	0.203	-13.59	11.92	4	0.499	142
0.487	0.465	0.046	12.78	15.80	1	0.202	101
0.916	0.071	0.011	-12.65	15.71	1	0.213	106
1	0	0	-12.87	16.51	1	0.208	107

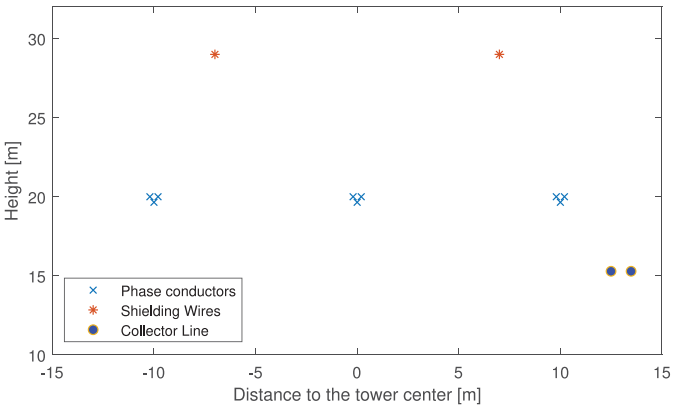

Fig. 10. Conductor geometry on the tower.

increase the induced voltage ($m_1 = 1$), the quantity of floating wires is reduced and the tuned reactor is seriously compromised.

With this, a clear trade-off between objectives is observed. Therefore, in the decision making process Fig. 9 can be used to select one solution according the specific needs of the project and the willing to sacrifice one or another objective.

Table IV describes the solution space, i.e., the physical characteristics of the solutions, also helps in the decision making process. In this case, the selection of the solution can be done based on the preferences for x_k, x_y, n_c, r_b, and t_c. For instance, if the major concern is the collector line height, solution one on Table IV should be chosen.

One possible solution is presented in Fig. 10, showing the collector and the transmission lines. The solution corresponds to the bold values at Tables III and IV. The solution chosen corresponds to a bundled-wire with 2 conductors of the number 101, a sag of 8.76 m, a tower height of 15.32 meters and 13 meters

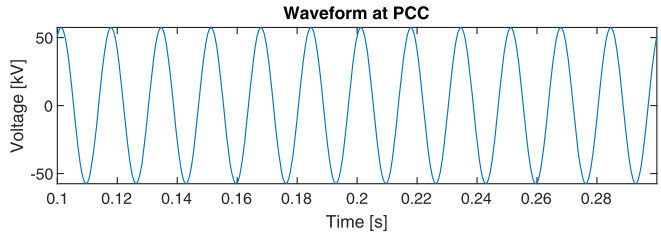

Fig. 11. Voltage waveform for a 100 kW at PCC.

of distance to the center of the transmission line. In this case, the selection is based on having a collector line with voltage in the range of 35 to 40 kV, tuning reactor between 25 to 35 H and cost between 50 and 150 $kUSD. As can be seen, the selected solution has a small number of conductors, low size bundle, and a regular pole height.

The final selection can be based on both spaces. However, it is normally performed based on the objective space, supported by the solution space.

In Fig. 11 the voltage waveform at PCC supplying 100 kW is presented. The high energy quality can be observed.

VI. FINAL CONSIDERATIONS

The use of floating wires as a way to electrify isolate communities poses some engineering challenges due to the nature of the problem. As presented in [13], because of the resonant circuit added to improve the voltage regulation on the rural load, the induced voltage on the collector line increases when the rural load increases. Therefore, once the target load is defined and inputted to the algorithm, the final solution depends on the induced voltage and the value of the tuned reactor. In the present project, the induced voltage selected for the collector line allows the use of regular isolation elements, that in this case are 69 kV elements.

Overall, this electrification technique allows attending load of hundreds of kW, but it is limited to the characteristics of the transmission line assets and the voltage levels of the collector line. Accordingly, the analysis of the rural load and the collector line length must be performed for each new case.

Regarding the decision to use the same span for the collector line, it avoids possible reductions of the distance between phase cables and floating wires in the event of horizontal movements caused by wind forces. However, an in-depth study must be carried out analyzing the variations in the tuning reactor, what will be presented in a future material.

As a complement to the protection system, spark gaps must be added at the terminals and middle point of the collector line. This method avoids overvoltages due to switching/lightning at both the host transmission line and the collector line. Since the spark gaps would be used in all collector line alternative, their price is not considered in the optimization model. In this sense, all fixed costs are not taken into account during the optimization process, such as maintenance costs.

Finally, since the reactor has a very high value, it is necessary to reduce it to regular size. In this way, the use of a transformer group is a viable solution [22].

VII. Conclusion

This paper presents a detailed mathematical model, solved with a genetic algorithm, to design an optimal collector line (CL) inside the right-of-way of a extra-high voltage transmission line. The system is used to extract small amount of energy from the electric field surrounding the host EHV transmission line. The algorithm optimizes the induced voltage at the floating CL wires, and minimizes the project total cost and the size of the reactor used for voltage regulation. The collector line was optimized by selecting the optimal position, bundle wires quantity, bundle radius and type of conductor.

The algorithm performance was tested for a collector system applied at a host 230-kV transmission line. It was verified the repeatability of solutions when using a population of $N = 500$ and 300 generations. Then, the weighting sum approach was used to observe the trade-off between objectives, performing more than 1000 simulations with random objective weights.

It was evidenced that if the goal is to reduce the tuned reactor, it is necessary to use a larger quantity of wires. However, the total project cost increased and the induced voltage reduced. On the other hand, a strong reduction of costs will produce poor values of induced voltage. In case of prioritizing the induced voltage, the height of collector line increases, and the number of wires in the collector line is reduced, resulting in a significant increase of the required tuned reactor.

The final choice of the geometry is a-posteriori decision of the designer, that can be based on the results of the objective and solution space. The selected collector system is a non-conventional generation system that extracts energy from high voltage transmission line electric field to attend small isolated communities that may leave dark days in the past.

References

[1] R. Horton, M. Halpin, and K. Wallace, "Induced voltage in parallel transmission lines caused by electric field induction," in *Proc. IEEE 11th Int. Conf. Trans. Distrib. Construct., Oper. Live-Line Maintenance*, Oct. 15–19, 2006.

[2] H. G. Sarmiento, R. de la Rosa, V. Carrillo, and J. Vilar, "Solving electric energy supply to rural areas: The capacitive voltage divider," *IEEE Trans. Power Del.*, vol. 5, no. 1, pp. 259–265, Jan. 1990.

[3] J. Wang, Y. Wang, X. Peng, X. Li, X. Xu, and X. Mao, "Induced voltage of overhead ground wires in 500-kV single-circuit transmission lines," *IEEE Trans. Power Del.*, vol. 29, no. 3, pp. 1054-1062, Apr. 2014.

[4] G. Kochan, K. Lenarczyk, K. Kiczkajło, and B. Dudek, "Replacement of existing ground wire with OPGW under live-line conditions new training polygon in Olsztyn," in *Proc. - 11th Int. Conf. Live Maintenance*, Budapest Hungary, 2014, pp. 21–25.

[5] R. Vasquez-Arnez, M. Masuda, J. Jardini, and E. Nicodem, "Tap-off power from a transmission line shield wires to feed small loads," in *Proc. IEEE/PES Transmiss. Distrib. Conf. Expo.: Latin America.*, Sao Paulo, Brazil, 2010, pp. 116–121.

[6] E. Iliceto, E. Cinieri, L. Casely-Hayford, and G. O. Dokyi, "New concepts on MV distribution from insulated shield wires of HV lines," *IEEE Trans. Power Del.*, vol. 4, no. 4, pp. 2130–2144, Oct. 1989.

[7] J. Ramos, A. Piantini, V. A. Pires, and A. D'Ajuz, "The Brazilian experience with the use of the shield wire line technology (SWL) for energy distribution," *IEEE Latin Amer. Trans.*, vol. 7, no. 6, pp. 650–656, Dec. 2009.

[8] R. Berthiame and R. Blais, "Microwave repeater power supply tapped from the overhead ground wire on 735 kV transmission lines," *IEEE Trans. Power App. Syst.*, vol. PAS-99, no. 1, pp. 183–184, Jan. 1980.

[9] L. Bolduc, B. Bouchard, and G. Beaulieu, "Capacitive divider substation," *IEEE Trans. Power Del.*, vol. 12, no. 3, pp. 1202–1208, Jul. 1997.

[10] L. Bolduc, S. Member, Y. Brissette, and P. Savard, "IVACE: A self-regulating variable reactor," *IEEE Trans. Power Del.*, vol. 19, no. 1, pp. 387–392, Jan. 2004.

[11] R. Blais, "Supplying fixed and stroboscopic," *IEEE Trans. Power App. Syst.*, vol. PAS-99, no. 1, pp. 181–182, Jan. 1980.

[12] F. Llanos, "Use of energy in the shielding wire as an alternative for feeding small loads [In Spanish]," *Comisión 2: "Energía y uso racional de Recursos" - Lima-Peru*, 1981.

[13] S. Chaves and M. C. Tavares, "Micro-loads electrification: Use of insulated shielding wires of a 500 kV transmission line," *Energy for Sustainable Development - Elsevier*, 2017.

[14] J. S. Chaves and M. Tavares, "Transient study of rural electrification using induced voltage at transmission lines' shielding," in *Proc. Int. Conf. Power Syst. Transients*, Seoul-South Korea, 2017. [Online]. Available: http://www.ipstconf.org/papers/Proc_IPST2017/17IPST098.pdf

[15] J. S. Chaves and M. C. Tavares, "Rural electrification using capacitive induced voltage on transmission lines' shield wires," in *Proc. IEEE PES Asia-Pacific Power Energy Eng. Conf.*, Xian-China, 2016, pp. 89–93.

[16] IEEE, "IEEE guide for the application of insulation coordination," *IEEE Standard 1313.2-1999*, p. i, 1999.

[17] ABNT, "NBR 5422 1985: Projeto de linhas aéreas de transmissão de energia elétrica," 1985. [Online]. Available: https://www.abntcatalogo.com.br/norma.aspx?ID=9416

[18] *IEEE Guide for Improving the Lightning Performance of Transmission Lines*, IEEE Std 1243-1997, pp. 1–44, Dec. 1997.

[19] Starr, Lloyd, and Peek, "An investigation of corona loss: Law of corona and dielectric strength," *J. Amer. Inst. Electr. Eng.*, vol. 46, no. 12, pp. 1457–1461, 1927.

[20] C. J. Miller, "The calculation of radio and corona characteristics of transmission-line conductors," *Trans. Am. Inst. Electr. Eng. Part III Power Appar. Syst.*, vol. 76, no. 3, pp. 461–472, 1957.

[21] M. Srinivas and L. M. Patnaik, "Genetic algorithms: A survey," *Comput.*, vol. 27, no. 6, pp. 17–26, Jun. 1994.

[22] J. S. Chaves and M. Tavares, "Analyzing rural electrification topologies based on induced voltage at insulated shielding wires," *IEEE Trans. Power Del.*, vol. 34, no. 1, pp. 53–62, Feb. 2019.